12

Marangoni Condensation Heat Transfer

Yoshio Utaka
Yokohama National University
Japan

1. Introduction

Marangoni condensation phenomena, which show the extremely high heat transfer coefficient in the dropwise condensation regime, occur due to surface tension instability of the condensate in the condensation of binary a vapor mixture of a positive system (i.e., one in which the surface tension of the mixture has a negative gradient with the mass fraction of the volatile component, such as water - ethanol and water - ammonium mixtures.) Marangoni dropwise condensation differ from so-called dropwise condensation which occurs only on the lyophobic surface and easily occurs on the wetting surface. This phenomenon was first reported by Mirkovich & Missen (1961) for a binary mixture of organic vapors. Ford & Missen (1968) demonstrated that the criterion for instability of a condensate liquid film. Fujii et al. (1993) experimentally investigated the condensation of water - ethanol mixtures in a horizontal tube and found that several different condensation modes such as dropwise and rivulets occur depending on concentration. Morrison & Deans (1997) measured the heat transfer characteristics of a water - ammonium vapor mixture and found that it exhibited enhanced heat transfer.

Utaka & Terachi (1995a, 1995b) measured the condensation characteristic curves and clarified that surface subcooling is one of the dominant factors in determining the condensate and heat transfer characteristics of Marangoni condensation although the effect of concentration of binary mixture was major factor deciding the condensation modes in most experimental reserches. Moreover, the effects of external conditions such as the vapor mass fraction (Utaka & Wang, 2004) and the vapor velocity (Utaka & Kobayashi, 2003) were investigated. Heat transfer was significantly enhanced at low mass fractions of ethanol in a water - ethanol mixture. Murase et al. (2007) studied Marangoni condensation of steam - ethanol mixtures using a horizontal condenser tube. Their results showed similar trends as those of (Utaka & Wang, 2004) for vertical surfaces.

On the other hand, the mechanisms of Marangoni condensation have also been studied. Hijikata et al. (1996) presented a theoretical drop growth mechanism for Marangoni dropwise condensation. They found that the Marangoni effect that occurs due to a difference in the surface tension plays a more important role than the absolute value of the surface tension in Marangoni condensation. Utaka et al. (1998) investigated the effect of the initial drop distance, which is the average distance of the initially formed drops grown from a thin flat condensate film that appears immediately after a drop departs. They clarified that the initial drop distance is closely related to the heat transfer

characteristics of Marangoni condensation. Further, Utaka & Nishikawa (2003a, 2003b) measured the thickness of condensate films on the tracks of departing drops and between drops by applying the laser extinction method. They found that the condensate film thickness was approximately 1 μm and that it is closely related to the initial drop distance and the heat transfer characteristics.
In this paper, the mechanisms and the heat transfer characteristics of Marangoni condensation phenomena are described on the basis of those researches.

2. General description of mechanisms and characteristics of Marangoni condensation phenomena

2.1 Outline of mechanisms and characteristics of Marangoni condensation phenomena

The conditions determining the condensate modes in condensation of binary mixtures depend upon the phase equilibrium relation between liquid and vapor and the magnitude relation between surface tension of two liquids. Marangoni condensation appears typically for the case of so-called positive system, in which the surface tension of more volatile component σ_L is lower than that of non-volatile component σ_H. Such a instability in the system of liquid evaporation was shown by Hovestreijit (1963) for the first time. The mechanism of Marangoni condensation was explained by Fujii et al. (1993) from the similar point of view as shown in Fig. 1. The thicker condensate liquid (point B in Fig. 1) pull the thinner condensate (point A) due to the surface tension difference occurred by the distributions of surface temperature and concentration of liquid. As a result, the irregular condensate thickness augmented and the irregular modes of condensate such as dropwise appear by the surface instability. The phase equilibrium ralation and the variation of surface tension against mass fraction for water – ethanol binary mixture, which is major test material as a positive system in this study, is shown in Fig. 2.
The major dominant parameters in Marangoni condensation are the concentration of vapor and the surface subcooling of condensing surface. Althoug the concentration of vapor was a main factor determining the condensation mode, in investigating the heat transfer characteristics of Marangoni condensation, surface subcooling was found to be the fundamental factor controlling the condensate modes by Utaka-Terachi (1995a, 1995b). In other words, the change in heat transfer coefficient showed strong non-linearity with condensate mode transition because the Marangoni dropwise condensation formed in the vapor-side appears over the wide range of surface subcooling, in addition to the change in diffusion resistance, which is inherent in the condensation of binary mixtures. The features of the condensation characteristic curves are summarized schematically in Fig. 3, in which the variations of heat flux q and heat transfere coefficient α aginst surface subcooling ΔT are shown. Table 1 shows the characters in the change in heat transfer codfficient. Alphabetical symbols in the figure and table denote characteristic points in the condensation characteristic curves. Points B and D are the steep increase point of heat transfer and the maximum heat transfer point, respectively. The condensate shows the dropwise mode in a wide range of surface subcooling, encompassing B and D, and the dropwise mode appears when approaching point D from B. With further increase of the surface subcooling, the minimum point of the heat flux and the point of inflection of the heat transfer coefficient (E) appear as the end point of the transition region.

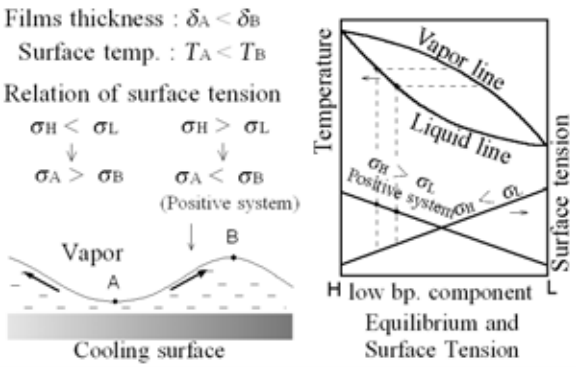

Fig. 1. Mechanisms of Marangoni condensation phenomena

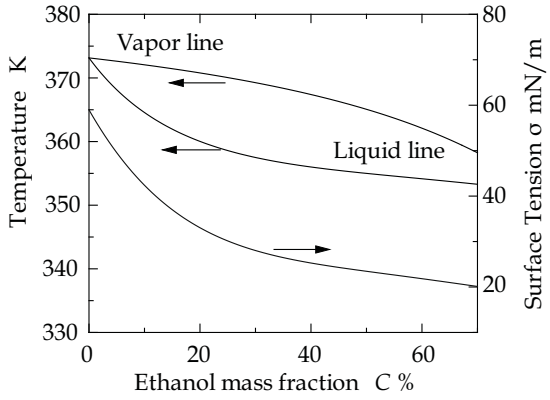

Fig. 2. Phase equilibrium relation and surface tension variation for water-ethanol mixtures

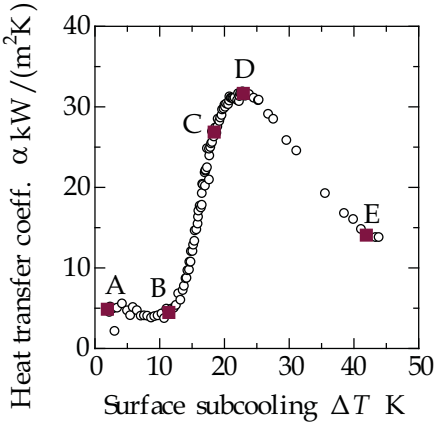

Fig. 3. Nature of condensation characteristic curves for Marangoni condensation

Domain	Characteristics
Smaller ΔT than steep increase pt. (B) (Vapor-side dominant region, A -B)	Small α Diffusion resistance dominant
Linear increase of α from pt. (B) to pt. (C) (Steep increase region, B -C)	Reduction of diffusion resistance Dropwise condensation
Departing from linear increase Maximum α pt. (D) Negative gradient region (Transition region, C -E)	Reduction of α
(Film region (E -))	Film condensation

Table 1. Nature of Marangoni condensation heat transfer

2.2 Marangoni dropwise condensation cycle

There are drop cycles in Marangoni dropwise condensation similar to dropwise condensation on a lyophobic surface. Since detailed aspects of condensate variation describe later in the relating sections, only the basic items are discussed here. First, just after sweeping by a departing drop in a typical condensation process, thin liquid condensate film remains. Next, the formation of initial drops commences along with the continuous condensation. Then, the drops grow with condensation and coalescences of drops. At the final stage of the cycle, some largest drops begin to depart due to the effect of external forces such as gravity and vapor flow and the new thin liquid film appears. Those cycles are repeated irregularly.

3. Experimental apparatus and methods common in measurements

Typical experimental apparatus and method common for Marangoni condensation experiments were shown next. A copper heat transfer block devised specifically for investigating phenomena with large heat flux and high heat transfer coefficients (Utaka & Kobayshi, 2003) was shown in Fig. 4. The heat transfer block having a cross-section of trapezoidal shape with notches was constructed in order to realize uniformity of surface temperature and large heat flux. The condensing surface had an area of 10 mm×20 mm. The copper block of one-dimensional rectangular column was also utilized for the cases realizing moderate heat flux. Oxidized titanium was applied to the condensing surface in order to achieve a wetting surface. In addition, impinging water jets from a bundle of thin tubes were used so as to provide high and uniform cooling intensity. A schematic diagram of the leak-tight experimental apparatus, intended to minimize the effects of non-condensing gas, is shown in Fig. 6 (Utaka & Wang, 2004). After passing through the condensing chamber (Fig. 5) in which the heat transfer block is placed, the vapor generated in the steam generator is condensed almost entirely in the auxiliary condenser. The condensate is returned to the vapor generator by the plunger pump via the flow measurement equipment. The vapor flow is in the same direction in which gravity acts, through a duct. Non-condensing gas is continuously extracted by the vacuum pump near the outlet of the auxiliary condenser. The inlet of the vacuum pump is cooled by an

electronic cooler to maintain a constant concentration in the vapor mixture, by maintaining low vapor pressure. The loop was divided into a high-pressure part and a low-pressure part bounded by the pressure adjusting valve and the return pump. The vapor pressure of the high-pressure-side is maintained at approximately 1 kPa above atmospheric pressure. The concentration of non-condensing gas in the vapor mixture is measured before and after the experiment. Another heat transfer block shown in Fig. 6 for the vapor concentration measurement is attached in the condensing chamber located downstream of the main heat transfer block.

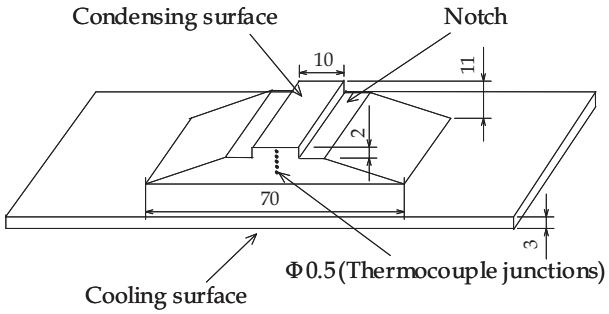

Fig. 4. Heat transfer block for large heat flux

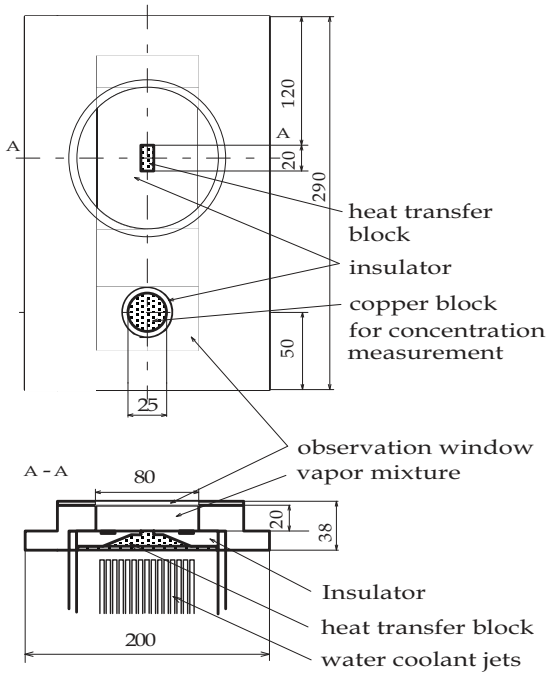

Fig. 5. Condensing chamber

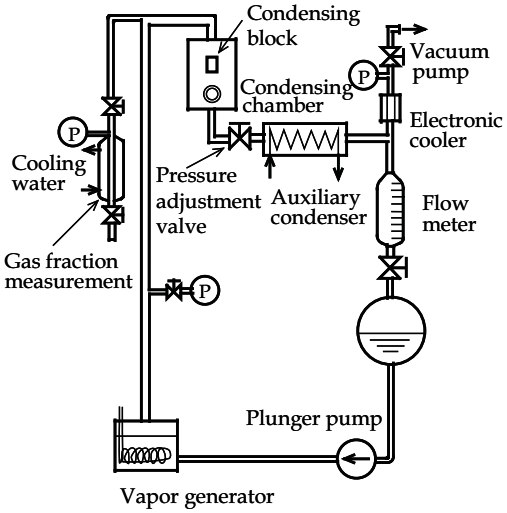

Fig. 6. Schematic diagram of experimental apparatus

After the vapor condition reaches the steady state, the condensation characteristic curves were measured continuously using a quasi-steady measurement in which the temperature of the cooling water was changed very slowly for a fixed concentration and fixed velocity of vapor. The aspect of condensate was observed and recorded through the glass window of the condensing chamber using a high speed camera to analyze the condensate characteristics.

4. Factors concerning mechanisms of Marangoni condensation

As described in Section 2, the irregurarity of condensate appears due to surface tenstion instability of the condensation system for binary mixtures of positive system in Marangoni condensation. Hijikata et al. (1996) performed the instability analyses and gave proof of Maragoni condensation phenomena theoretically. In this section, the dominant factors concerning the mecanism of heat transfer in Marangoni condensation is discussed.

4.1 Relation between initial drop distance and heat transfer

(a) Observation and measurements of drop formation

The observation and measurement of the process of formation and growth of condensate drops commenced after the sweeping action by the departing drops were carried out for four ethanol mass fractions of vapor c, i.e., c = 0.07, 0.17, 0.37 and 0.52 under constant vapor velocity at atmospheric pressure (Utaka, et al. 1998). Figure 7 (a) - (c) shows the photographs taken by the high speed camera. Figure 8 (a) shows the condensation heat transfer characteristic curves measured simultaneously with the taking photographs. The local maximum drops sizes increased with increasing distance from the up-flow side peripherals of the departing drops, which are shown as the largest drops in the images, because the time elapsed from the sweep motions by departing drops increased with the distance owing to the limited velocity of the drop departure. It is also seen that almost no droplets existed at the relatively thin belt-wise areas just next to the up-flow side peripherals of the departing drops. The small droplets appeared at the next areas. Hence, the initial drops form from the

thin liquid film and then grow by condensation and coalescences as reported in the observation of Hijikata et al. (1996) by making the uniform sweeping over the whole surface. It could be understood that the drop sizes nearest to the peripherals of the departing drops varied with the surface subcooling.

The initial drop distance d_i, which is the distance between adjoining drops forms after the sweeping, were adopted as parameters determining the characteristics against the variation of the ethanol concentration and the surface subcooling. Here, the reason for adopting the initial drop distance to decide the characteristics of drop formation is as follows. It is difficult to determine the minimum drop size because the unevenness of thin condensate film and drop shape are not distinguishable each other. On the contrary, since the initial drop distance does not change until an occurrence of a first coalescence, it can be defined certainly.

The variations of initial drop distance measured are shown in Fig. 8(b). Since the elapsed time after the end of sweep changes along the track of the departing drop as described above, the drop sizes varies along the departure direction. Therefore, the distance between the neighboring drop centers in the direction of the departing drop peripheral was adopted

(a) ΔT = 15.2 K (b) ΔT = 18.3K (c) ΔT = 29.5 K

Fig. 7. Aspect of condensate (c =0.37)

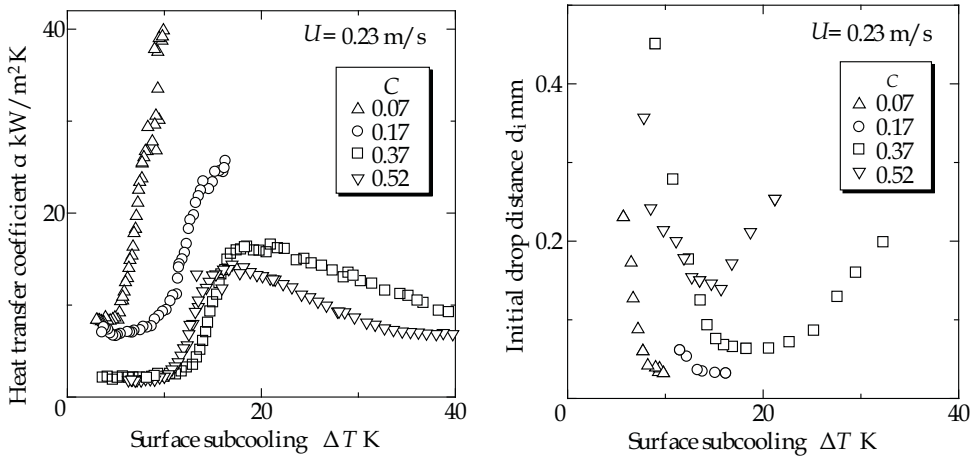

(a) Heat transfer characteristic curves (b) Variation in initial drop distance

Fig. 8. Relation among aspect of condensation, heat transfer characteristic curve, and initial drop distance

as the initial drop distance. As is evident from Fig. 8(b), the initial drop distances depend markedly on the surface subcooling in the Marangoni dropwise condensation. The U-shaped curves having minima were obtained for c = 0.37 and 0.52 since the measurement of the whole regions of the surface subcoolings were achieved. The curves until the minima were obtained for c = 0.07 and 0.17 as same subcooling regions as the characteristic curves. The ratio of least to greatest initial drop distances for each concentration changed widely and was in the range of 2 to 7. It is notable that the surface subcooling at the minimum of the initial drop distances nearly coincides with those at the maximum heat transfer coefficient for each concentration.

The smallest drops, which is nearly equal to the sizes of initial drop distances, were quite larger than those of dropwise condensation on a lyophobic surface and were 0.03 mm to 0.15 mm in this experimental range. Thus, the initial drop distance depended considerably on the ethanol concentration and surface subcooling. That is, the initial drop distance decreased with decreasing ethanol concentration and the maximum is about 5 times larger than the minimum. The minimum diameters of drops measured by Fujii et al (1993) were 0.2 mm and 0.05 mm for c = 0.48 and 0.34, respectively, and are ranged in those measurements. However, since their conditions of the surface subcooling were unknown as well as the concentrations are different from this measurement, it is difficult to get detailed comparison. Therefore, it indicates the possibility that the reduction of the thickness of the thin condensate film among drops together with the decrease of the initial drop distance and the approaching of the spherical shape is given by the increase of the driving force of the Marangoni effect.

4.2 Condensate film thickness

(a) Apparatus for measuring condensate film thickness

The entire experimental system, composed of the vapor loop, condensing chamber, cooling system, which are similar to those shown in Section 3, and laser extinction measurement system, is shown in Fig. 9 (Utaka & Nishikawa 2003a, 2003b).

Lambert's law (Eq. 1) was used for determining the condensate liquid thickness. Where, A is the laser exstinction coefficient, I_0 and I are the intensities of incident light and of transmission light, respectively, and δ is the optical path length.

$$\delta = -A^{-1} \times \log\left(I \,/\, I_0\right) \tag{1}$$

Since the extinction coefficient A is unknown and depends upon the mass fraction of the liquid mixture through which the laser beam passes, and was measured prior to the measurement of film thickness. The helium-neon laser beam, having 3.39 μm of 2.6 mm in diameter, is transformed to parallel light of 53 mm in diameter by the beam collimator lens. The beam is concentrated by passing through a condenser lens made from optical silicon. The beam waist is defined at the thin liquid layer of the mixture. The transmitted laser beam, which is partially absorbed by the test liquid enclosed in a quartz glass gap, is converged by the quartz glass lens. The transmitted light intensity I is measured by the detector (light reception area of 3 × 3 mm², response time of 1 ~ 3 μs) made of lead selenide. The incident light intensity I_0 is measured under the same conditions of transmitted light intensity without the test liquid. The diameter of the laser beam is approximately 30 μm at the test liquid.

The aspect of the condensate was photographed by a high-speed digital camera synchronously with the condensate film thickness measurement in order to confirm correspondence with the condensate behavior.

(b) Condensate behavior and variation in condensate film thickness

Simultaneous measurement of condensate film thickness and observation of condensate behavior during the formation of the initial drops commenced after the departing drops swept by, under four ethanol vapor mass fractions c of 0.11, 0.21, 0.30, and 0.40, and a constant vapor velocity of 0.7 m/s. Figures 10 (a) and (b) show the images of condensate behavior and the variations of condensate thickness as measured from light transmittance for c = 0.30. Figure 10 (a) shows the aspect of condensate appearing after departing drops swept by, and figure 10 (b) shows variations in condensate thickness immediately after the departing drops swept by. Here, t = 0 was determined arbitrarily, and the variation in liquid thickness and the image coincide with each other. The relatively large dark region on the right-hand side of each image denotes the departing drop, and the light-colored area is thin condensate film at t = 0 ms. Condensate thickness is non-uniform; i.e., the droplets grew rapidly from a flat thin film that appeared after the departing drops swept by. The measuring position irradiated by the laser beam is highlighted as a circle measuring about 30 μm in diameter. After the measuring position was covered by the departing drop at t = 0 ms, the thin film observed as the minimum condensate thickness immediately after sweeping at t = 6 ms by the movement of the departing drop towards the lower right-hand corner. At t = 28 ms, the thickness was measured at the drop having diameter of less than 0.2 mm. Thus, good correspondence between the variation of measured value and the aspect of condensate is confirmed. In this case, the measured minimum condensate thickness was 1.3 μm. These results confirm that a thin liquid film having a thickness of around 1 μm remains after sweeping and that the heat transfer surface was always covered by liquid in Marangoni dropwise condensation.

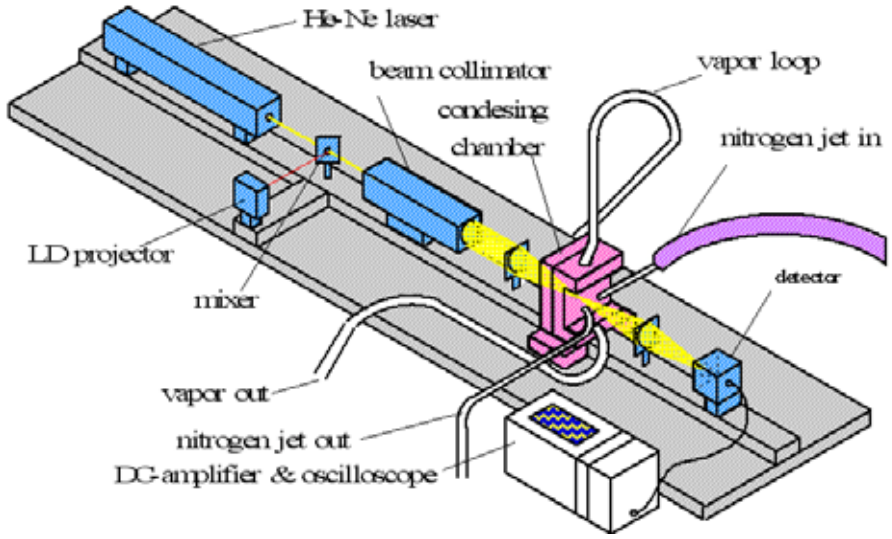

Fig. 9. Experimental apparatus for measuring condensate film thickness

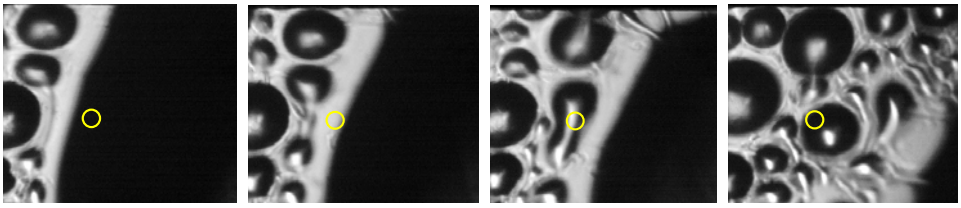

(a) Variation of condensate aspect

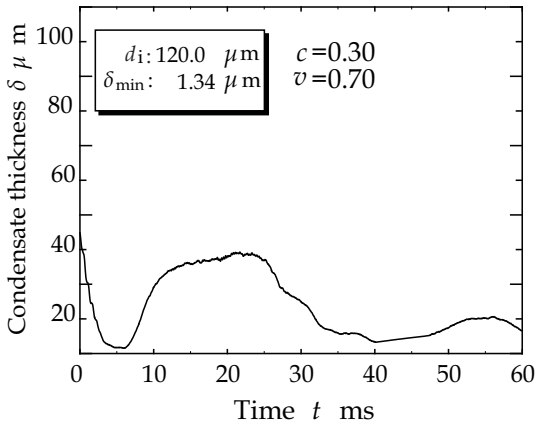

(b) Variation of condensate thickness

Fig. 10. Aspect of condensation and condensate thickness for c = 0.30 and δ_{min} = 1.34 μm

Figures 11 (a),(b),(c), and (d) show the relations between the minimum condensate film thickness δ_{min} appearing immediately after departing drops swept by in the Marangoni condensation cycle and the initial condensate thickness measured from the simultaneously obtained images for four ethanol vapor concentrations, i.e.; c = 0.11, 0.21, 0.30, and 0.42. Initial drop distance was adopted as the averaged value for at least several drop departures. For all vapor concentrations, minimum condensate thickness decreased as initial drop distances decreased in association with increasing surface subcooling. For the higher ethanol vapor concentrations of 0.30 and 0.42 shown in Figs. 11 (c) and (d), respectively, the minimum drop distances decreased linearly with decreasing initial drop distance in association with increased surface subcooling. Afterwards, the minimum thickness became minimum. Both the initial drop distance and the minimum condensate thickness increased with further increase in cooling intensity. Since, as shown in section 4.1, the maximum heat transfer coefficient appeared in a region near the minimum initial drop distance, and the return portion of the curve; i.e., the region near the minimum initial drop distance and the smallest minimum condensate thickness, should correspond to the maximum heat transfer point in the condensation characteristic curve. The minimum condensate thickness for the vapor ethanol mass fractions of 0.30 and 0.42 was very thin; that is, 1.2 μm and 1.5 μm, respectively. Minimum condensate thickness showed a tendency to decrease with decreasing vapor ethanol concentration. The minimum values of minimum condensate

thickness for the mass fraction of ethanol vapor of 0.11 and 0.21 were about 1 μm, because of the limit of cooling intensity. In the present study, larger surface subcooling in the thinner ethanol concentration region associated with very large heat flux was difficult to realize, because quartz glass and the jet of evaporated liquid nitrogen gas were used as a heat transfer surface and a coolant, respectively. Therefore, minimum condensate thickness could not be measured near the region of minimum value. Linear curves fitted by the least squares

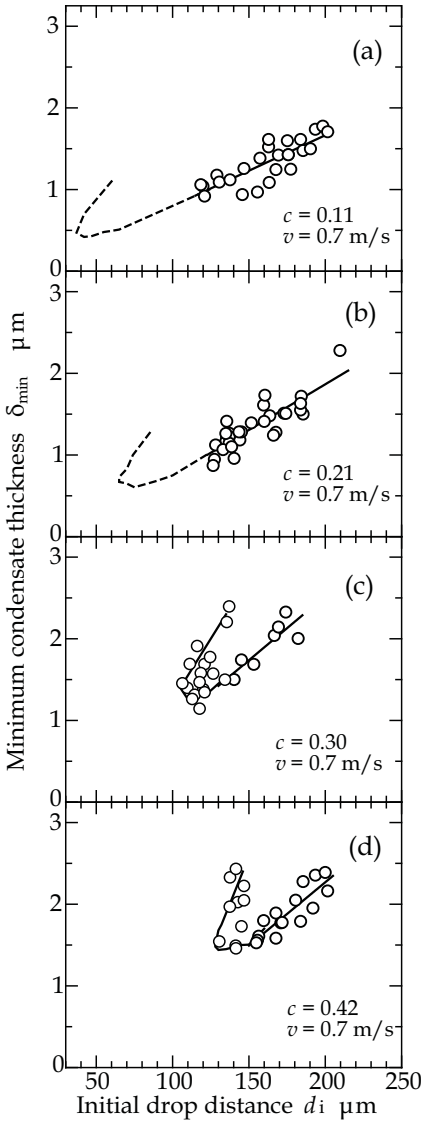

Fig. 11. Variation of minimum film thickness against initial drop distances after sweeping by departing drops

method to the data showing the linear changes had slopes of 0.0087, 0.011, 0.016, and 0.016 for ethanol mass fractions of 0.11, 0.21, 0.30, and 0.42, respectively, and tended to increase with ethanol concentration. The dotted lines in Figs. 11 (a) and (b) were predicted on the basis of the characteristic features of the curves shown in Figs. 11 (c) and (d) and the previous results shown in section 4.1. Although results do not lend themselves to detailed quantitative discussion, minimum thickness can be predicted to decrease with increasing ethanol concentration and to reach less than 0.5 μm.

The results of this section and section 4.1 clarified that close coincidence exists among the features of heat transfer variation in the condensation characteristic curves and their characteristic quantities, such as initial drop distance, departing drop diameter, and minimum condensate thickness, whose minimum is attained at the surface subcooling near maximum heat transfer coefficient. Similar features of these characteristic quantities in relation to ethanol concentration were also obtained. Therefore, the variations in heat transfer coefficient in the condensation characteristic curves were shown to correspond to the changes in the distributions of surface tension differences, which are the driving force of condensate irregularity in Marangoni condensation. Most likely, the maximum driving force appears in the vicinity of peak value of heat transfer coefficient and the thinning of the condensate thin film. Therefore, the heat transfer is enhanced near the maximum heat transfer coefficient point when the thinning of the condensate film with the augmentation of surface tension difference and the decrease in diffusion resistance, which is discussed in next section, occur.

4.3 Vapor-side diffusion characteristics

For Marangoni condensation, the condensate resistance based on the condensate aspect and the mass diffusion resistance in the vapor-side are important fundamentally in controlling the condensation characteristics. This phenomenon consists of the unsteady process whereby the condensate thickness and the vapor concentration change due to the variation of the condensate mode. An analysis of the vapor-side diffusion resistance is required in order to explain the detailed mechanism. The relation between the condensate aspect and the condensation characteristic was previously reported in former sections.

Here, a model approximating the process just after sweeping by a departing drop in a typical condensation process was considered along with the diffusion resistance (Wang & Utaka, 2005). Rapid condensation occurs with the beginning of sweeping of the heat transfer surface by a departing drop. The concentration distribution proceeds due to rapid condensation from the initial situation where the heat transfer surface is covered by a large drop with comparatively lower heat transfer and nearly uniform concentration distribution. By solving a one-dimensional unsteady diffusion equation derived from the idealized process described above numerically, the thermal conductance variation of the vapor-side for a process in which the condensation occurs swiftly from uniform concentration is investigated.

The vapor-liquid interface temperature is given as a boundary condition in order to consider only the conductance in the vapor phase. In addition, since the condensate film thickness was very thin, approximately 1 μm, as describe in seciton 4.2, in the surface subcooling range near the maximum heat transfer coefficient, the thermal resistance of the condensate film is small and the surface temperature of the condensate liquid is near that of the heat transfer surface. The basic equation, the boundary conditions, and the initial condition can be written as:

$$\frac{\partial C}{\partial t} + V\frac{\partial C}{\partial y} = D\frac{\partial^2 C}{\partial y^2} \tag{2}$$

$$y = 0 : C = C_I \tag{3}$$

$$(\rho D\frac{\partial C}{\partial y})_I = (C_{IL} - C_I)m \tag{4}$$

$$m = \rho V \tag{5}$$

$$y = \infty : C = C_\infty \tag{6}$$

$$t = 0 : C = C_\infty \tag{7}$$

where C is the ethanol mass fraction of the water-ethanol vapor mixture, D is the diffusivity between water and ethanol, V is the velocity of the vapor flowing into the heat transfer surface due to the condensation, ρ is the vapor density, m is the condensation rate, and C_I, C_{IL} and C_∞ are the ethanol concentrations of vapor and liquid in the vapor-liquid interface and the bulk vapor concentration, respectively. The thermal conductance H and the non-dimensional temperature difference ΔT^* in the vapor phase are defined respectively as:

$$H = Lm/(T_S - T_I) \tag{8}$$

$$\Delta T^* = (T_S - T_I)/(T_S - T_L) \tag{9}$$

where L is the latent heat of condensation, T_s and T_L are the dew point and boiling point tempetatures, respectively, corresponding to the vapor concentration C_∞ in the phase equilibrium diagram of water and ethanol, and T_I is the temperature of the vapor-liquid interface.

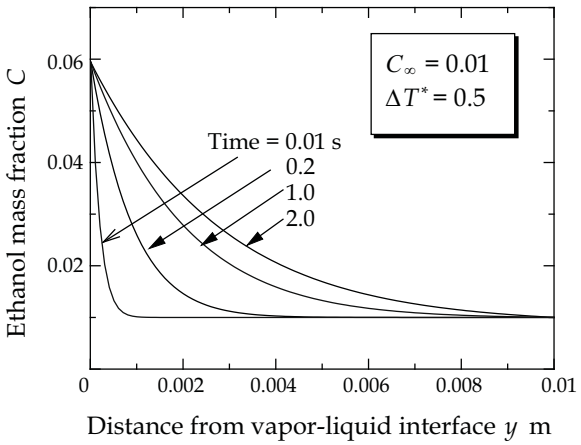

Fig. 12. Variation of distribution of mixture vapor concentration with time

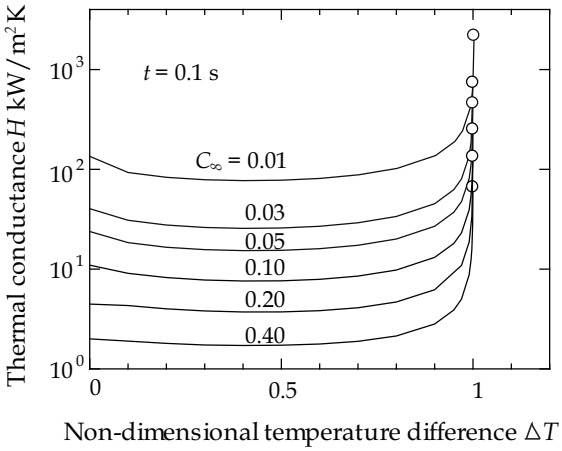

Fig. 13. Variation of thermal conductance with respect to non-dimensional temperature difference in the vapor layer (t = 0.1 s)

Figure 12 shows the time variation of ethanol mass fraction distribution in the vapor phase. It is seen that the thickness of different concentration region becomes thicker with time. Figure 13 shows the variation of thermal conductance with the non-dimensional temperature difference in the vapor phase for the different bulk vapor mass fractions, calculated when the time equals 0.1 seconds. Assuming a similar distribution of the condensate shape, the period of frequency between drop departures is inversely proportional to the heat flux. Therefore the characteristic time is dependent on that period. Also, the maximum heat flux of such a diffusion process is different for different vapor concentrations. However, for convenience, the thermal conductance at a fixed time is compared in order to examine the character of the variation in the condensation characteristic curve and its characteristic points. Since the sweeping period by the departing drop is approximately 0.1~0.2 s at the maximum heat transfer coefficient on the condensation characteristic curves, the calculation result for this time was adopted herein.

As a characteristic of the vapor-side diffusion resistance, the heat flux tends to increase rapidly for any vapor concentration when the non-dimensional temperature difference approaches 1.0 (i.e. the vapor-liquid interface temperature approaches the boiling point), because the compositions of the condensation and the bulk vapors also approach each other. The decrease in the diffusion resistance in the vapor-side due to the decrease in ethanol concentration improved the heat transfer performance. This is thought to be one of the reasons why a relatively high maximum heat transfer coefficient appears in the low-vapor-concentration region.

5. Heat transfer characteristics of Marangoni condensation

The factors affecting the characteristics of heat transfer in Marangoni condensation is investigated in this section. That is, the effects of given external conditions such as vapor concentration, vapor velocity and non-condensing gas concentration. Also, the effect of surface subcooling varying the cooling intensity in detail.

5.1 Effects of surface subcooling and vapor concentration

(a) Condensation characteristic curves

The condensation characteristic curves under atmospheric pressure and at vapor velocitie *U* of 1.5 m/s for a considerable range of ethanol concentrations are shown in Figs. 14 (a) and (b) (Utaka & Wang, 2004). Since film condensation appeared in all subcooling regions for pure water vapor, monotonical change, which is a feature of ordinary film condensation heat transfer, was exhibited. In contrast, a common trend was observed for ethanol vapor mass fractions larger than 0.05%. That is, the qualitative features of each curve showed a common characteristic change having heat flux and heat transfer coefficient maxima as shown in section 2.

From these characteristic curves, excellent heat transfer were confirmed, whereby the heat transfer coefficient maxima shifted to the smaller subcooling region and the values at the maxima were very high at low ethanol concentrations, with the exception of the extremely low ethanol concentrations of 0.05% and 0.1%. In addition, in the low ethanol concentration range, the dependencies of the condensation heat transfer characteristics on the vapor concentration and the surface subcooling become greater, and the gradient of the characteristic curves at the smaller subcooling range increases.

As indicated in a previous report (Utaka & Terachi, 1995a), the realization of excellent heat transfer characteristics is likely due to the following. Since the temperature difference between the boiling point line and dew point line decreases as the ethanol concentration of

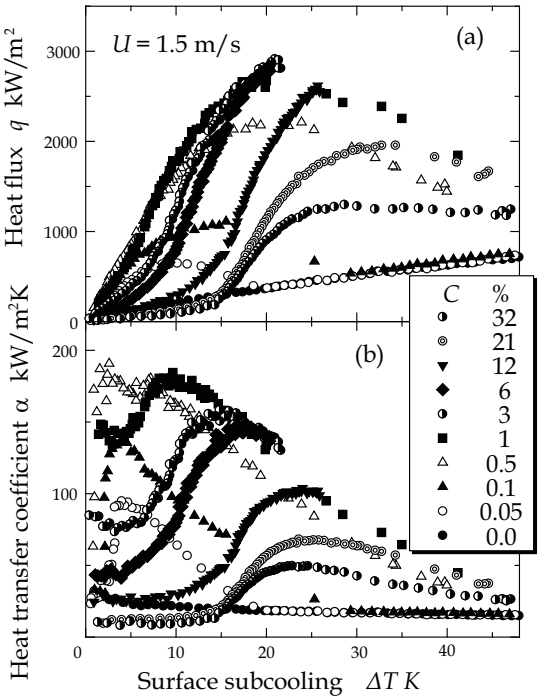

Fig. 14. Condensation heat transfer characteristic curves (*U* = 1.5 m/s)

the vapor mixture decreases, the subcooling region of condensation controlled by the diffusion resistance in the vapor-side becomes narrower due to the nature of vapor-liquid equilibrium relation. Moreover, since the difference between ethanol concentrations of the vapor in bulk and at the vapor-liquid interface is small and the variation of surface tension with respect to the concentration is large, higher heat transfer conductance is realized.

In order to evaluate the condensation characteristic curves quantitatively, we examined the heat transfer quantities at the commencement points of the steep increase in heat transfer, the maximum heat transfer coefficient and maximum heat flux, as well as the condensing surface subcooling. Figure 15 shows the variation of surface subcooling with respect to vapor ethanol concentration at the commencement points of the steep increase in heat flux and the heat transfer coefficient for vapor velocity of 0.4 and 1.5 m/s. The steep increase in heat transfer is confirmed to have begun approximately when the temperature of the heat transfer surface reached the dew point line temperature. The surface subcooling at the commencement point of the steep increase almost coincided with the temperature difference between the boiling point line and the dew point line in the vapor-liquid equilibrium relation. However, the surface subcooling at the steep increase point is slightly higher than the temperature difference between the dew point and the bubble point in the vapor-liquid phase equilibrium, and is almost constant in the low-concentration range of less than 3% ethanol.

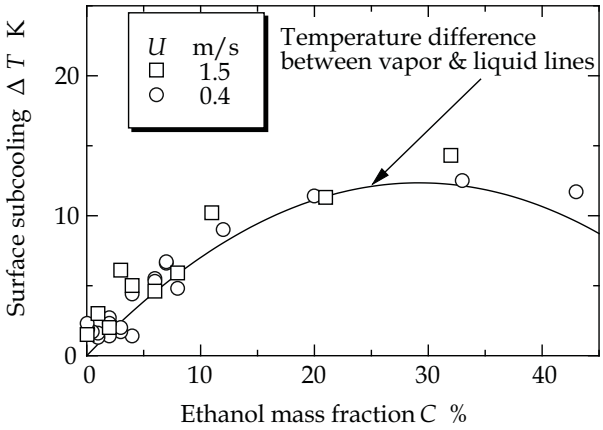

Fig. 15. Surface subcooling at the steep increase point of heat transfer

Figures 16 (a) and (b) show the changes in the maximum heat flux and heat transfer coefficient, respectively, with the condensing surface subcooling, the maximum values of which appear in the region of low ethanol concentration. When the vapor velocity was 0.4 m/s, a maximum heat flux of approximately 1.7 MW/m² appeared at an ethanol concentration of nearly C = 6%. The surface subcooling at the maximum value of heat flux increased monotonically with respect to the vapor concentration, and the rate of increase was relatively high in the low-concentration range. When the vapor velocity was 1.5 m/s, a maximum heat flux could not be directly obtained due to insufficient cooling intensity and excessive heat flux. Assuming a similar trend in behavior as for the vapor velocity of 0.4 m/s, the maximum heat flux at vapor velocity of 1.5 m/s was estimated to be approximately

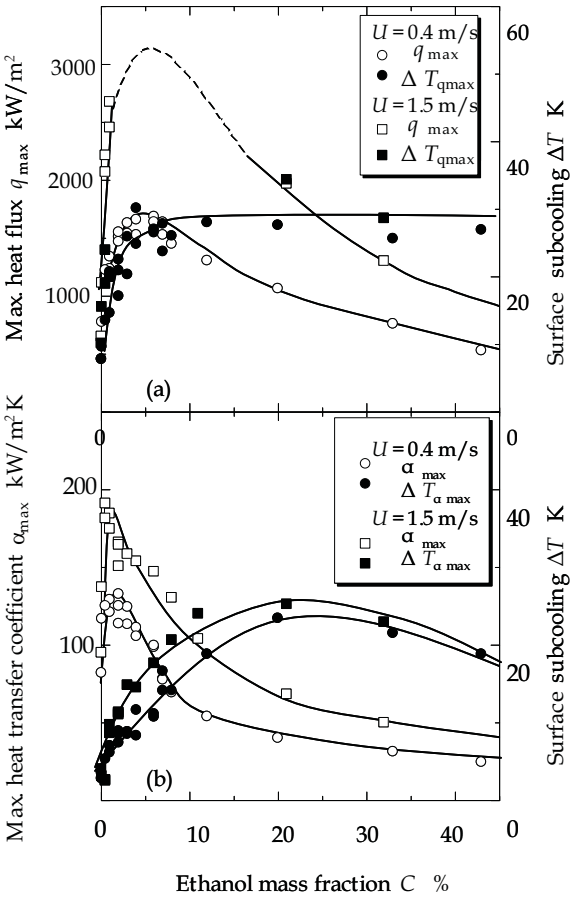

Fig. 16. Characteristics of maximum points of heat transfer (a) Maximum heat flux, (b) Maximum heat transfer coefficient

3 MW/m², as indicated by the dotted line in Fig. 15 (a). As shown in Fig. 15 (b), the maximum heat transfer coefficients appeared at an ethanol concentration of approximately C = 1%, and were 0.12 MW/m²K and 0.18 MW/m²K for vapor velocities of 0.4 m/s and 1.5 m/s, respectively. In addition, the subcooling at the maximum heat transfer coefficient showed some variation, with a peak that appeared at a vapor concentration of approximately 20%.

(b) Promotion of steam condensation by addition of ethanol

We examine the promotion of condensation heat transfer by adding ethanol to water. Figure 17 shows the variation of the condensation heat transfer coefficient of the vapor mixture normalized by that of pure steam with respect to the subcooling, for a vapor velocity of 0.4 m/s. For all vapor concentrations, the maximum shifted slightly from that of the characteristic curve toward larger subcooling. This is due to the lowering of the heat transfer coefficient for pure steam with the increase in subcooling. The condensation heat transfer

was improved over almost the entire measured subcooling region for ethanol concentrations of less than approximately 6%. On the other hand, when the ethanol concentration of the vapor mixture was higher than 12%, the ratio of condensation heat transfer of the vapor mixture is smaller than that of steam in the low-subcooling region, but is higher in the subcooling region larger than that of the commencement point of steep increase. As discussed in section 3.4, the mutual relationship of the Marangoni driving force on the condensate and the diffusion resistance in the vapor phase in the condensation of binary vapor mixtures determines the condensation characteristics. The decrease in condensation heat transfer coefficient due to the diffusion resistance of the vapor-side is relatively small in the case of $C \leq 6\%$ for low ethanol concentration. In the case of $C \geq 12\%$, as the diffusion resistance is the controlling factor, the condensation heat transfer coefficient was reduced even in the dropwise mode.

Figure 18 shows the relationships between the ethanol concentration of the vapor mixture and the maximum value of the ratio of the heat transfer coefficient of the vapor mixture, α_{peak}, to steam, α_0, with respect to the surface subcooling. For an ethanol concentration of approximately 1%, the addition of ethanol improves the condensation heat transfer coefficient of the mixture, compared to steam, by a factor of approximately six at a vapor velocity of 0.4m/s, and by a factor of approximately eight at a vapor velocity of 1.5 m/s. In addition, for vapor concentrations of 0.05% and 0.1% (ethanol concentrations of the liquid mixture were 0.005% and 0.01%, respectively), which are very low, the ratios of the heat transfer coefficients reached 3.5~5.5, and the subcooling is in the relatively small temperature difference range of approximately 3~5 K. Thus, the addition of a very small amount of ethanol is expected to promote the heat transfer process for a comparatively small temperature difference and at sustained high heat transfer coefficient regardless of the nature of the condensation surface.

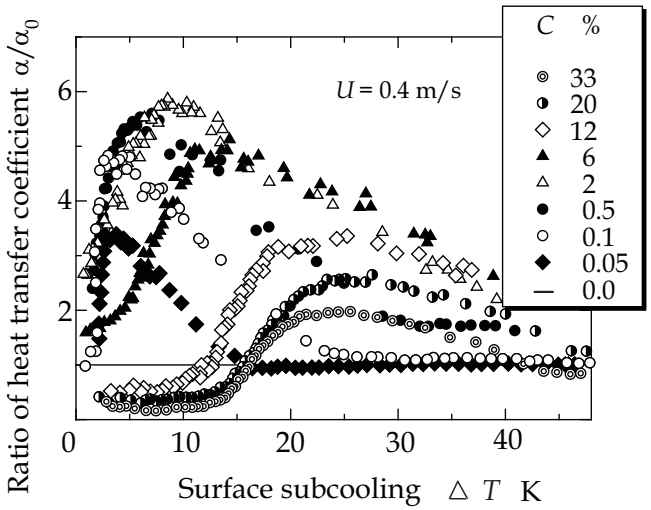

Fig. 17. Ratio of the condensation heat transfer coefficient of the mixture vapors to that of pure steam, with respect to surface subcooling

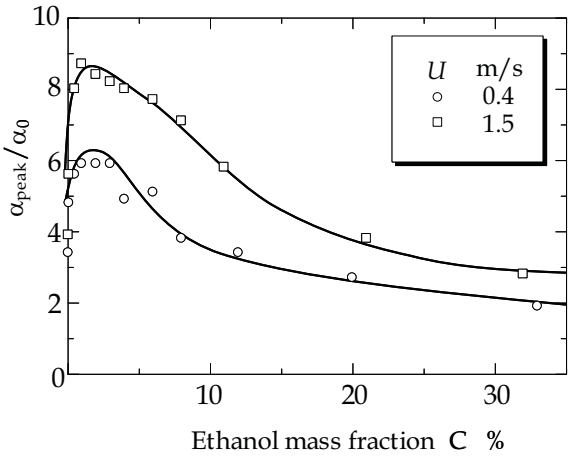

Fig. 18. Variation of the peak ratio of the condensation heat transfer coefficient of the mixture vapors to that of pure steam with respect to the ethanol concentration in the mixture vapors

5.2 Effect of vapor velocity

Condensation characteristic curves were measured for three ethanol mass fractions of water-ethanol vapor mixture c = 0.09, 0.32, 0.53. The results for each of the concentrations are shown in Figs. 19(a) and (b) for c = 0.09, 0.32 (Utaka & Kobayashi, 2003). The vapor velocity was varied from 0.3 to 45 m/s for c = 0.32 and 0.53 and from 0.3 to 68 m/s for c = 0.09. The region near the maximum heat tlux could not be measured when the vapor velocity was over 18 m/s for c = 0.09 because of the limited cooling intensity. The condensation heat transfer coefficient increased remarkably throughout whole subcooling region with the increase in vapor velocity under all conditions. Moreover, the surface subcooling in which the maximum heat transfer coefficient appeared moved towards the smaller subcooling-side with the increase in vapor velocity. The maximal value of heat transfer coefficient is very high for the thinnest ethanol concentration of c = 0.09 and is about 200 kW/m^{2}K for vapor velocity over 18 m/s. As describe before, thermal resistance of Marangoni condensation is composed of the resistance layers of diffusion in steam-side and the condensate. As shown in Table 1, with increasing surface subcooling, the dominant heat transfer resistances shifts from diffusion layer in the vapor phase to condensate layer. There are two effects of increase in vapor velocity, that is, weakening of the vapor-side resistance and condensate resistance due to the decrease in the largest droplet size in dropwise condensation region. Therefore, the characteristic measured from the above-mentioned experiment is related to these features. First, the increase in heat transfer coefficient with the vapor velocity is remarkable in the region where surface subcooling is relatively small. For example, the heat transfer coefficient increased by nearly tenfold at the steep increase point (the point B in Fig. 3) from 5 kW/m2K to 45 kW/m2K with the change in vapor velocity from 0.8 m/s to 45 m/s for c = 0.32. Therefore, the vapor velocity affects the heat transfer characteristic at the steep increase point which is mainly controlled by the diffusion resistance, because the effect of the vapor flow influences steam-side diffusion resistance. Next, the maximum heat trasfer coefficient increases nearly 2 times from 45 kW/m2K to 80 kW/m2K under the same

condition. Similar tendencies are also found in the other two concentration conditions. In general, since the diffusion resistance in vapor layer is smaller than the condensate thermal resistance near the surface subcooling at the point of maximum heat transfer coefficient, and the condensate resistance is also smaller compared to that at smaller surface subcooling region because of the appearance of clear dropwise mode. Especially, when the vapor velocity increases, the decrease of condensate resistance caused by a reduction in the size of the largest drop on the heat transfer surface becomes remarkable and is similar to that in so-called dropwise condensation process on a lyophobic surface. With increased vapor velociity, maximum heat transfer coefficient point shifts to smaller subcooling. This is due to lower condensate surface temperature caused by reduced average condensate thickness.

Figures 20 (a) and (b) show the relations among the maximum heat transfer coefficient as a representative point showing the feature of condensation characteristic curve, the vapor velocity and the departing drop diameter. In this region, since thermal resistance of the condensate is the main factor over the vapor-side thermal resistance, it is worth comparing the effect of vapor velocity with the result (Tanasawa et al. 1973) of dropwise condensation on a lyophobic surface where the effect of drop conduction is important. While the relation between maximum heat transfer coefficient and vapor velocity in Marangoni condensation is similar for all of the conditions, those are greatly different from that of dropwise condensation. Thus, the difference in the dependecies of departing drop size to the vapor velocity observed between two phenomena is due not only to the droplet shape but also to the condition of drop peripheral. That is, while there is a three phase interface of solid, vapor and liquid in dropwise condensation on a lyophobic surface, a continuous condensate film exists among the drops so that there is no boundary between drop and condensate film in Marangoni dropwise condensation. Figure 20 (b) shows the change of the maximum heat transfer coefficient against the departing drop diameter. The line fitted by using least square method in the figure was applied to the above measuring points for vapor velocity greater than 0.8 m/s. Since each gradient of the curves almost agrees with that for dropwise condensation on a lyophobic surface, it can be seen that the effect of departing drop diameter on the heat transfer coefficient is similar to each other. Similar trends of dependencies on departing drop diameters both for the maximum heat transfer coefficient in Marangoni condensation and the heat transfer coefficient of dropwise condensation is considered here.

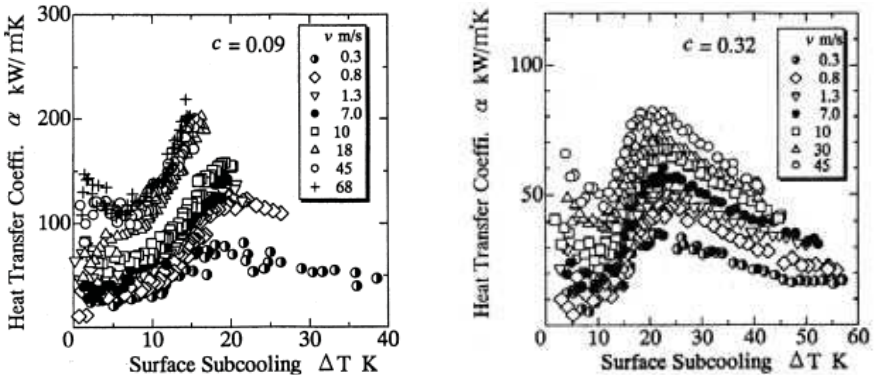

(a) c = 0.09 (b) c = 0.32

Fig. 19. Condensation characteristic curves

It has been clarified that comparatively large drops on condensing surface in dropwise condensation on a lyophobic surface works as a hindrance to heat transfer and that the major part of heat transfer occurs through small drops. Therefore, considering that the condensate resistance is dominant and that the dropwise mode appears at the point of maximum heat transfer coefficient, it can be understood why the exponents agree with one another because relatively large drops work as heat resistance and the thin condensate between the dorps are taking on the major heat transfer.

5.3 Effect of non-condensing gas

In order to realize the lowest non-condensing gas concentration, the leak-tight vapor loop, which is shown in Fig. 5, was first sealed off from the atmosphere (Wang & Utaka, 2005). In order to change the non-condensing gas concentration, a structure in which nitrogenous gas could be added to the vapor mixture as non-condensing gas was adopted. The amount and the stability of the added non-condensing gas were observed by measuring the flow of nitrogenous gas using a flow meter.

Figures 20 (a) and (b) shows the condensation characteristic curves of heat transfer coefficient under ethanol mass fractions of the vapor mixture of 0.01 and 0.45, respectvely. The condensation heat transfer performance improves with the decrease in the concentration of the non-condensing gas for vapor mixtures of all ethanol concentrations. In particular, the condensation heat transfer performance of the vapor mixture can be improved by further reducing the concentration of the non-condensing gas, even in cases of very small non-condensing gas concentration.

As shown in Fig. 3, Marangoni condensation characteristic curves can be divided into four domains: the domain controlled by the diffusion resistance of the vapor-side, the rapid decrease domain of the diffusion resistance, and the domains controlled by dropwise and filmwise condensations. For each domain, since the main factor governing the heat transfer is different, the degree of the effect of the non-condensing gas on the condensation heat transfer should also be different.

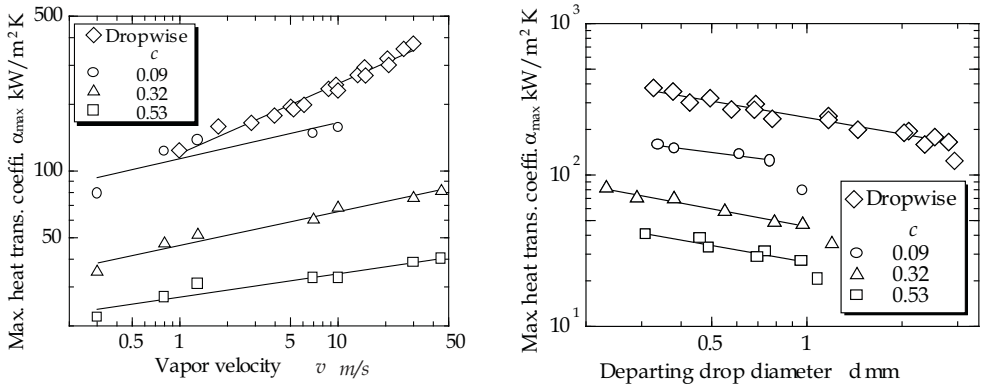

Fig. 20. Heat transfer characteristics at point of maximum heat transfer coefficient;
(a) Variation of maximum heat transfer coefficient against vapor velocity; (b) Variation of maximum heat transfer coefficient against departing drop diameter

First, in the domain controlled by the diffusion resistance of the vapor-side (domain A-B in Fig. 3), the diffusion resistance of the vapor-side is large and the amount of condensate is comparatively small due to the small heat flux. Therefore, the effect of the non-condensing gas is comparatively small. Particularly, for the case in which the vapor ethanol concentration is high (Fig. 21 (b)), this tendency is clear. Next, in the rapid decrease domain of the diffusion resistance (domain B-C), as the diffusion resistance of the vapor-side decreases rapidly while the condensate is maintained dropwise, the condensation heat flux increases suddenly. Corresponding to this change, the effect of the non-condensing gas increases suddenly. As seen in Fig. 21, with the increase of the non-condensing gas concentration, the condensation characteristic curve showed the tendency to decrease from the commencement point of the steep increase, and the drop became large with the increase in surface subcooling. Moreover, in the domain controlled by the dropwise condensation (domain C-E), since the condensate maintains the dropwise aspect and the diffusion resistance on the vapor-side is small, the heat transfer coefficient showed was high. Hence, the domain is a region in which the effect of non-condensing gas on Marangoni condensation appears easily. These figures show that the decrease in heat transfer coefficient or heat flux due to the existence of the non-condensable gas becomes remarkable around the peak value of the condensation characteristic curve, and is comparatively large. For example, in the case of the ethanol concentration in vapor mixture of C_e = 0.01, when the non-condensable gas concentration was increased from 15×10^{-6} to 494×10^{-6}, the peak value of the heat transfer coefficient was reduced by about 35% and the peak value of the heat flux was reduced by about 40%. Even at other vapor ethanol concentrations, the decrease of the peak value of the heat transfer coefficient or the heat flux due to the increase in the non-condensing gas concentration to the degree mentioned above is between approximately 30%-50%. The reasons for this are as follows. 1) In this domain, since the condensation heat flux is comparatively high, the non-condensing gas accumulates easily, therefore the diffusion resistance layer of the non-condensing gas form easily. 2) In this domain, both the heat transfer resistance in the condensate and the diffusion resistance due to the low-boiling-point component in the vapor mixture are small. In other words, the diffusion resistance caused by the non-condensing gas becomes relatively large in comparison with other heat

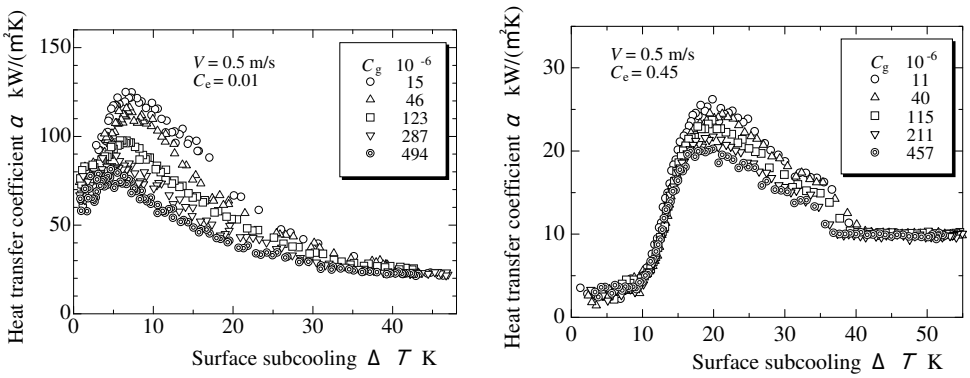

Fig. 21. Effect of non-condensing gas in Marangoni condensation curve

transfer resistance in the condensation process. Furthermore, for this domain, as the driving force that makes the condensate irregular, the temperature difference formed on the surface of the condensate decreases again after an increase and gradually approaches zero (the condensate becomes filmwise). As a result, the variation of the heat transfer resistance in the condensate with respect to the surface subcooling having a tendency to decrease in the initial stage and increase again after reaching the minimum around the point of peak heat transfer coefficient. Hence, the effect of non-condensing gas on Marangoni condensation becomes greatest around the subcooling at which the peak heat transfer coefficient. Finally, in the domain controlled by the filmwise condensation (the area to the right of point E), as the condensate becomes filmwise, the diffusion resistance formed by the non-condensing gas and the low-boiling-point component in the vapor mixture is relatively small in the condensation process, the effect of the non-condensable gas is not readily apparent.

These figures also indicate that the effect of the non-condensing gas is different under different ethanol concentrations of vapor mixture. Specifically, in the case of the low ethanol concentration of vapor mixture, the heat flux characteristic curve of which has a strongly nonlinear shape, the nonlinearity became weak and the heat flux peak becomes indistinct with the increase in non-condensing gas concentration. The effect of the non-condensable gas becomes stronger because the diffusion resistance of the low-boiling-point component in the condensation process is small when the ethanol concentration of the vapor mixture is low. On the other hand, in the case of the larger ethanol concentration, the effect of non-condensing gas is weaker because of the existence of larger vapor-side heat transfer resistance due to much non-volatile (ethanol) concentration as seen in Fig. 21 (b).

6. Concluding remarks

The mechanisms and heat transfer characteristics of Marangoni condensation phenomena, which show the extremely high heat transfer coefficient in the dropwise condensation regime and occur due to surface tension instability of the condensate in the condensation of a binary vapor mixture of a positive system, are investigated mainly on the basis of the researches of author's group. That is, the general description of mechanisms and characteristics of Marangoni condensation phenomena, Marangoni dropwise condensation cycle, experimental apparatus and methods common in measurements, factors concerning the mechanisms of marangoni condensation (Relation between initial drop distance and heat transfer, condensate film thickness, and vapor-side diffusion characteristics), and the heat transfer characteristics of Marangoni condensation (effects of surface subcooling, vapor concentration, vapor velocity and non-condensing gas) were discussed.

7. References

Ford, J.D. and Missen, R.W. (1968). On the Conditions for Stability of Falling Films Subject to Surface Tension Disturbances; the Condensation of Binary Vapor, *Can. J. Chem. Eng.*, Vol. 48, pp. 309-312.

Fujii, T., Osa, N., Koyama, S. (1993). Free Convective Condensation of Binary Vapor Mixtures on a Smooth Horizontal Tube: Condensing Mode and Heat Transfer Coefficient of Condensate, *Proc. US Engineering Foundation Conference on Condensation and Condenser Design*, St. Augustine, Florida, ASME, pp. 171-182.

Hijikata, K., Fukasaku, Y., Nakabeppu, O. (1996). Theoretical and Experimental Studies on the Pseudo-Dropwise Condensation of a Binary Vapor Mixture, *Journal of Heat Transfer*, Vol. 118, pp. 140-147.

Hovestreijdt, J. (1963). The Influence of the Surface Tension Difference on the Boiling of Mixture, *Chem. Eng. Sci.*, Vol. 18, pp. 631-639.

Mirkovich, V.V. and Missen, R.W. (1961). Non-Filmwise Condensation of Binary Vapor of Miscible Liquids, *Can. J. Chem. Eng.,* Vol. 39, pp. 86-87.

Morrison, J.N.A. and Deans, J. (1997). Augmentation of Steam Condensation Heat Transfer by Addition of Ammonia, *International Journal of Heat and Mass Transfer*, Vol. 40, pp. 765–772.

Murase, T., Wang, H.S., Rose, J.W. (2007). Marangoni condensation of steam-ethanol mixtures on a horizontal tube, *International Journal of Heat and Mass Transfer*, Vol. 50, pp. 3774-3779.

Tanasawa, I., Ochiai, J., Utaka, Y. and Enya, S. (1976). Experimental Study on Dropwise Condensation Process (Effect of Departing Drop Size), *Trans. JSME*, Vol. 42, No. 361, pp. 2846-2853.

Utaka, Y. and Terachi, N. (1995a). Measurement of Condensation Characteristic Curves for Binary Mixture of Steam and Ethanol Vapor, *Heat Transfer-Japanese Research*, Vol. 24, pp. 57-67.

Utaka, Y. and Terachi, N. (1995b). Study on Condensation Heat Transfer for Steam-Ethanol Vapor Mixture (Relation between Condensation Characteristic Curve and Modes of Condensate), *Transactions of Japan Society of Mechanical Engineers*, Series B, Vol. 61, No. 588, pp. 3059-3065.

Utaka, Y., Kenmotsu, T., Yokoyama, S. (1998). Study on Marangoni Condensation (Measurement and Observation for Water and Ethanol Vapor Mixture), *Proceedings of 11th International Heat Transfer Conference*, Vol. 6, pp. 397-402.

Utaka, Y. and Kobayashi, H. (2003). Effect of Vapor Velocity on Condensation Heat Transfer for Water-Ethanol Binary Vapor Mixture, *Proceedings of 6th ASME-JSME Thermal Engineering Conference*.

Utaka, Y. and Nishikawa, T. (2003a). An Investigation of Liquid Film Thickness during solutal Marangoni Condensation Using a Laser Absorption Method (Absorption Property and Examination of Measuring Method) , *Heat Transfer – Asian Research*, Vol.32, No.8, pp.700-711.

Utaka, Y. and Nishikawa, T. (2003b). Measurement of Condensate Film Thickness for Solutal Marangoni Condensation Applying Laser Extinction Method, *Journal of Enhanced Heat Transfer*, Vol. 10, No. 1, pp. 119-129.

Utaka, Y. and Wang, S. (2004). Characteristic Curves and the Promotion Effect of Ethanol Addition on Steam Condensation Heat Transfer, *International Journal of Heat and Mass Transfer*, Vol. 47, pp. 4507-4516.

Wang, S. and Utaka, Y. (2005). An Experimental Study on the Effect of Non-condensable Gas for Solutal Marangoni Condensation Heat Transfer, *Experimental Heat Transfer*, Vol. 18, No. 2, pp. 61-79.

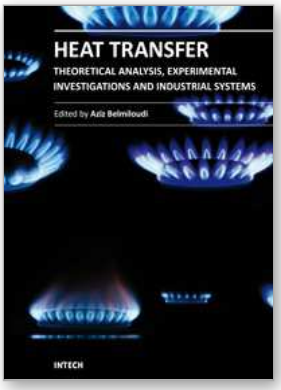

Heat Transfer - Theoretical Analysis, Experimental Investigations and Industrial Systems

Edited by Prof. Aziz Belmiloudi

ISBN 978-953-307-226-5
Hard cover, 654 pages
Publisher InTech
Published online 28, January, 2011
Published in print edition January, 2011

Over the past few decades there has been a prolific increase in research and development in area of heat transfer, heat exchangers and their associated technologies. This book is a collection of current research in the above mentioned areas and discusses experimental, theoretical and calculation approaches and industrial utilizations with modern ideas and methods to study heat transfer for single and multiphase systems. The topics considered include various basic concepts of heat transfer, the fundamental modes of heat transfer (namely conduction, convection and radiation), thermophysical properties, condensation, boiling, freezing, innovative experiments, measurement analysis, theoretical models and simulations, with many real-world problems and important modern applications. The book is divided in four sections : "Heat Transfer in Micro Systems", "Boiling, Freezing and Condensation Heat Transfer", "Heat Transfer and its Assessment", "Heat Transfer Calculations", and each section discusses a wide variety of techniques, methods and applications in accordance with the subjects. The combination of theoretical and experimental investigations with many important practical applications of current interest will make this book of interest to researchers, scientists, engineers and graduate students, who make use of experimental and theoretical investigations, assessment and enhancement techniques in this multidisciplinary field as well as to researchers in mathematical modelling, computer simulations and information sciences, who make use of experimental and theoretical investigations as a means of critical assessment of models and results derived from advanced numerical simulations and improvement of the developed models and numerical methods.

InTech Europe
University Campus STeP Ri
Slavka Krautzeka 83/A
51000 Rijeka, Croatia

InTech China
Unit 405, Office Block, Hotel Equatorial Shanghai
No.65, Yan An Road (West), Shanghai, 200040, China
中国上海市延安西路65号上海国际贵都大饭店办公楼405单元

Phone: +385 (51) 770 447
Fax: +385 (51) 686 166
www.intechopen.com

Phone: +86-21-62489820
Fax: +86-21-62489821